SSRG International Journal of Electrical and Electronics Engineering
ISSN: 2348-8379/ https://doi.org/10.14445/23488379/IJEEE-V12I11P115

Volume 12 Issue 11, 182-199, November 2025

Original Article

Human Activity Recognition with Topological Data Analysis Using Machine Learning Algorithms

Sunil Chaudhari[1*], Sanjay Kumar Singh[1], Sandeep Singh Senghar[2], Bhupesh Kumar Singh[1]

[1]*Amity University Rajasthan, Jaipur, Rajasthan, India.*
[2]*Dr. APJ Abdul Kalam University, Indore, MP, India.*

**Corresponding Author : sunil.chaudhari7@gmail.com*

Received: 11 September 2025 Revised: 12 October 2025 Accepted: 15 November 2025 Published: 28 November 2025

Abstract - *In the computer vision field, Human motion analysis is a significant research topic, as confirmed by an extensive range of applications like medical assistance, video surveillance, and virtual reality. Human motion analysis concerns the tracking, detection, and recognition of human behaviors and activities. Topology-based approaches have, in recent times, begun to come forward in the human action analysis field. These kinds of techniques are sometimes integrated with Machine Learning (ML) strategies, like Support Vector Machine (SVM) or a Convolutional Neural Network (CNN). In this work, a topology-aided Human Activity Recognition (HAR) method is developed using various ML methods, like Multilayer Perceptron (MLP), K Nearest Neighbor (KNN), Decision Tree, CNN, SVM, and Random Forest. From the time series data, topological features, like persistent landscape, Betti curve, Persistent images, Wasserstein amplitude, and Persistent Entropy, are extracted. Using the extracted features, the ML methods, Random Forest, SVM, CNN, Decision Tree, KNN, and MLP are used to recognize the human activities. Here, the overall analysis states that the CNN model attained better accuracy, recall, precision, and F1-score with the values of 98.3, 98.3, 96.9, and 98. Also, it is noted that the maximum accuracy of about 99% is attained for the watch_accel_score_personal label by the proposed method.*

Keywords - *Human activity recognition, Human motion analysis, Topological data analysis, Machine learning.*

1. Introduction

Body motion analysis of humans has been an attractive field due to its diverse applications, including medical diagnostics, athletic performance evaluation, human-machine interface, and virtual reality. Generally, in the analysis, three features of research directions are considered of human body motion, such as estimating and tracking the parameters of motion, human body structure verification, and motion activity recognition [5]. Moreover, Human motion analysis is a significant area of applied computer science with a lot of practical applications. Among these applications, medical and disability assistance, sports and health surveillance, gaming, and human-computer interaction are the most important. MoCap is represented as the process of human motion registration. To carry out this registration, several sensors are utilized that depend on the specific MoCap techniques, such as IMUs, video cameras, and others. For further analysis, it is processed to create a motion feature, which is helpful after collecting motion data. Motion is designed as a multi-dimensional time series in that each time series indicates a certain part of the body's coordinates in numerous scenarios. Nonetheless, these biological activity measurements may be diverse among individuals even if they carry out similar actions. This is because every person has somewhat diverse body flexibility and proportions that impact their motion trajectories. In addition, similar actions might be carried out with diverse speeds; thus, recognition of human action is a serious problem and presents issues of digital signal classification [7].

Topology mainly deals with the shape of the data. The view of shape is a basic concept in the evaluation of human insight. Shape displays many wonders and emphasizes multifaceted structures and interconnections in data. Not like conventional techniques, TDA is hypothesis-free, having no parameters or choice of coordinates. TDA needs point clouds of data, comprising pairwise distances with no scale, number of neighbors, or noise bound. TDA is 3-3 Models, three techniques (mapper, homology, classification), three properties or ideas (Compressed Representation, Stretch or Deformation Invariance, Coordinate Invariance), with three advantages (speed, accuracy, and defensibility). In HAR, data generated is unstructured, noisy, sparse, unclean, heterogeneous, high-dimensional, and messy. Conventional analytics is a slow, iterative procedure, has a few missing insights, and is dependent on expert individuals (Analysts and data scientists) inquiring the right questions of data and processing it. Generally, TDA is a relatively advanced field of

study that employs topological ideas to categorize and analyze data. The basis of TDA is the idea that the values are driven by meaning, and that data has shape and meaning.

Recently, AI, chiefly ML, has developed speedily regarding data analysis and computing that normally permits the applications to function in an intelligent way [23]. Generally, ML presents systems with the capability to learn and improve from experience automatically without being specially programmed and is usually indicated as the most well-liked recent technology [24]. In most daily HAR tasks, ML techniques might rely heavily on heuristic manual feature extraction. Generally, it is restricted by human domain knowledge, and Machine Learning (ML) is a subset of approaches that learn and adjust from data and subsequently take or recommend actions. ML permits companies to segment conventional data into significant groupings, recognize main segmentation features and attributes, determine patterns and anomalies, and accurately classify new data points as they reach their destination. There are two primary classes of ML approaches: unsupervised and supervised models. By utilizing a training data set, supervised learning designs predictive approaches to generate a function that can precisely infer outputs while presented with new input data. Moreover, the hidden structure in data can be identified by unsupervised learning, and it employs only the input data content and does not identify the expected outcome [25].

This research proposes a topology-based HAR approach based on different ML models, such as Random Forest, SVM, CNN, Decision Tree, KNN, and MLP. Topological features like persistence images, Wasserstein amplitude, persistent entropy, persistent landscape, and Betti curve are extracted from time series data by TDA. These are then utilized to train the ML models to identify and classify human actions, identifying intricate temporal patterns and enhancing recognition performance.

The major objectives of the proposed work are stated as:

1. To create an ML-aided HAR method using Random Forest, SVM, CNN, Decision Tree, KNN, and MLP.
2. Various topological features, like Persistent Entropy, Wasserstein amplitude, persistent landscape, and Betti curve from the persistence diagram, are used so that these features assist the recognition procedure to be effective.
3. To analyse the performance of the model, several metrics, such as accuracy, recall, precision, and f-measure, are employed.

2. Literature Review

This section states prior studies and research associated with HAR with TDA using ML algorithms. Cheng Xu et al. [1] designed a DL approach, named InnoHAR, based on the integration of RNN and INN. The waveform data of multi-channel sensors E2E was considered as input of the approach. Additionally, the Inception-like phases extracted the multi-dimensional features by employing several kernel-based convolution layers, which were integrated with GRU. Time series features were comprehended, which made complete usage of data characteristics to finish the classification tasks. Finally, the investigational analysis revealed that the model exhibited better performance and possessed better generalization performance on the most extensively utilized public datasets. Kun Xia et al. [2] presented a DNN that integrated convolutional layers with LSTM. The activity features were extracted by the model and automatically classified with some technique parameters. LSTM is a variation of the RNN approach that is highly appropriate for processing the temporal series. Here, using the mobile sensors, raw data were gathered and subjected to a two-layer LSTM, which was followed by convolutional layers. Additionally, to replace the fully connected layer, a GAP layer was used after the convolution to lessen the parameter count. After the GAP layer, batch normalization was augmented to increase the convergence, and evident outcomes were obtained.

Shengqin Wang et al. [3] developed a TCA-GCN for dynamically learning temporal as well as spatial topologies and competently aggregating topological features in diverse temporal as well as channel dimensions for skeleton-based action detection. To learn the channel aggregation phase, the phase of the temporal dimensional feature was used by the temporal aggregation phase to effectively integrate the spatial dynamic channel manner topological features with temporal dynamic topological features. Additionally, the multi-scale skeletal features on temporal modelling are integrated with an attention model, where they are extracted. Javier Lamar Leon et al. [4] developed a topological model to monitor human activities. This technique creates a security alarm. Initially, using thresholding and background subtraction, a stack of human silhouettes was glued via their gravity center, forming a 3D digital binary image. Next, diverse orders of simplices were used on a simplicial complex attained from the 3D binary image that captured relations between the human body parts while walking. At last, in accordance with each other, a topological signature was extracted from persistence illustrations. In order to present a similarity range amongst topological signatures, a cosine similarity measure was employed.

I.-Cheng Chang and Chung-Lin Huang et al. [5] designed a technique to examine the motion of human walking. This model comprised three modules: the pre-processing model, the technique construction module, and the motion analysis module. Finally, the experimentation phase revealed that the model not only verified the characteristics of motion of the human body but also identified the motion type of the input image series. At last, the synthesized motion sequences were exhibited for verification. Here, a skeleton-based model was utilized to verify the motion of the human, and also, the motion type was described by the HMM and posture patterns.

Umar Islambekov et al. [6] introduced a geometry-oriented approach based on the upcoming tools of TDA in the change point recognition model. The most important basis was that the alternate points were probably related to changes in geometry over the data generation procedure. When the TDA applications for change point detection were potentially extensive, topological concepts were integrated with conventional non-parametric approaches for change point detection. Specifically, a geometry-oriented model aspires to improve the detection accuracy of distributional regime shift positions.

Marcin Żelawski and Tomasz Hachaj [7] presented an approach based on TDA for human action recognition and motion capture (kinematic) processing. A human action regarding the topological features was characterized in contradiction to conventional techniques. Based on topological persistence, the recognition process is stable to perturbations. Here, the techniques presented in this work were exhibited efficiently with the human action recognition task, even on the complicated classes of motion observed in karate approaches. Adelie Garin and Guillaume Tauzin [8] presented a method for employing TDA in ML tasks on grayscale images. To create an extensive range of topological features, persistent homology was applied by utilizing a point cloud obtained from an image. Moreover, this topological ML pipeline was exhibited as an extremely appropriate dimensionality reduction by using it in the MNIST digits dataset. Moreover, a feature selection was performed, and their correlations were studied when presenting an instinctive interpretation of their significance, which was appropriate for both ML and TDA.

Angelo Trotta et al. [26] examined the fundamental problems in HAR by conceiving, developing, and testing edge-based HAR frameworks on resource-limited IoT devices using SOM for activity identification. A feature selection methodology was introduced before training to drive down the computational cost and data size of the SOM, which corresponds with wearable IoT hardware limitations. FL methods were also investigated so as to permit new users to take advantage of SOM models learned from other datasets. The federated EE-aware HAR system was executed on a wearable IoT device and tested by employing both advanced and experimental datasets. Shiwen Lan et al. [27] investigated a deep neural strategy, MnasNet, for HAR. The model was adapted through parameter fine-tuning with an enhanced IFT. Through the integration of MnasNet strengths with the optimization superiority of IFTT, the solution outperformed in terms of accuracy and efficiency. Experimental benchmark tests on standard datasets validated the performance superiority of the MnasNet/IFTT model in tasks of HAR. Lingyue Hu et al. [28] presented an improved classification resilience to adversarial attacks by utilizing the adversarial loss concept, thus enhancing reliability in adversarial settings. Graph construction using MST effectively captured intricate relationships between nodes that depicted various sections of the human anatomy. Moreover, the computation of gradients efficiently accelerated training convergence and reduced the vanishing gradient issue prevalent in DL networks.

2.1. Challenges

Some current feature extraction models and HAR based on DL have been widely investigated in the literature. According to the review of the previous section, topologically based methods mainly deal with the recognition of simple, periodic actions like walking, running, bicycling, and waving. These methods tend to need more techniques from ML and dynamical systems theory for them to be highly effective. One of the primary challenges in HAR is the proper classification of complex, aperiodic movements, which is critical for medical rehabilitation applications. This classification should be invariant to variations in execution speed, slight inconsistencies in movement, personal physical attributes, and other subject-related factors because mistakes in recognition or execution can have serious adverse outcomes. The raw data from HAR sensors is usually time-series in nature, non-stationary, non-linear, intrinsic, and high-dimensional, and hence prone to pattern drift with time. Furthermore, the involvement of several wearable sensors, whose position and orientation are not fixed, introduces noise and complexity, typically leading to compromised model performance. Posing as a remarkable challenge is extracting effective and discriminative features from this data. Due to variations in classification methods based on accuracy and computational expense, it is crucial to develop methods that are invariant to sensor orientation and location, preferably using coordinate- and parameter-free approaches, to successfully address the variability and complexity found in time-series sensor data.

3. Proposed Methodology

This section details the proposed HAR method using several ML techniques with TDA. Here, a technology is required that can have a compact depiction on a low-dimensional manifold, be able to detect emergent behaviors, and can take the system into its globality. Time series data has recurrent behavior or chaotic behavior. TDA can extract features from such dynamical systems, such as Betti curves, persistent landscapes, persistent images, etc. Persistent homology from TDA has the property of being coordinate-free. The placement of sensors does not affect the time series featurization using persistent homology. Persistent homology is a dimensionality reduction strategy; it maps the higher-dimensional time series to a low-dimensional manifold. So, it is easy to train the model with fewer dimensions. In the proposed work, TDA, specifically persistent homology, is applied to the given dataset, which is in the form of a time series. Here, the dataset is mapped to topological space, and then, the global topological features, like the Persistent images, Wasserstein amplitude, Persistent Entropy, persistent landscape, and Betti curve for extracting features, are analyzed. Next, intrinsic features and standard features are

also considered with TDA features. All the features are merged, and topological layers are applied in a deep learning model, which would predict the user's physical activity with sufficient confidence. Additionally, the detection of change points in the user's physical task is the focus of this work. Figure 1 illustrates the block diagram of the HAR model.

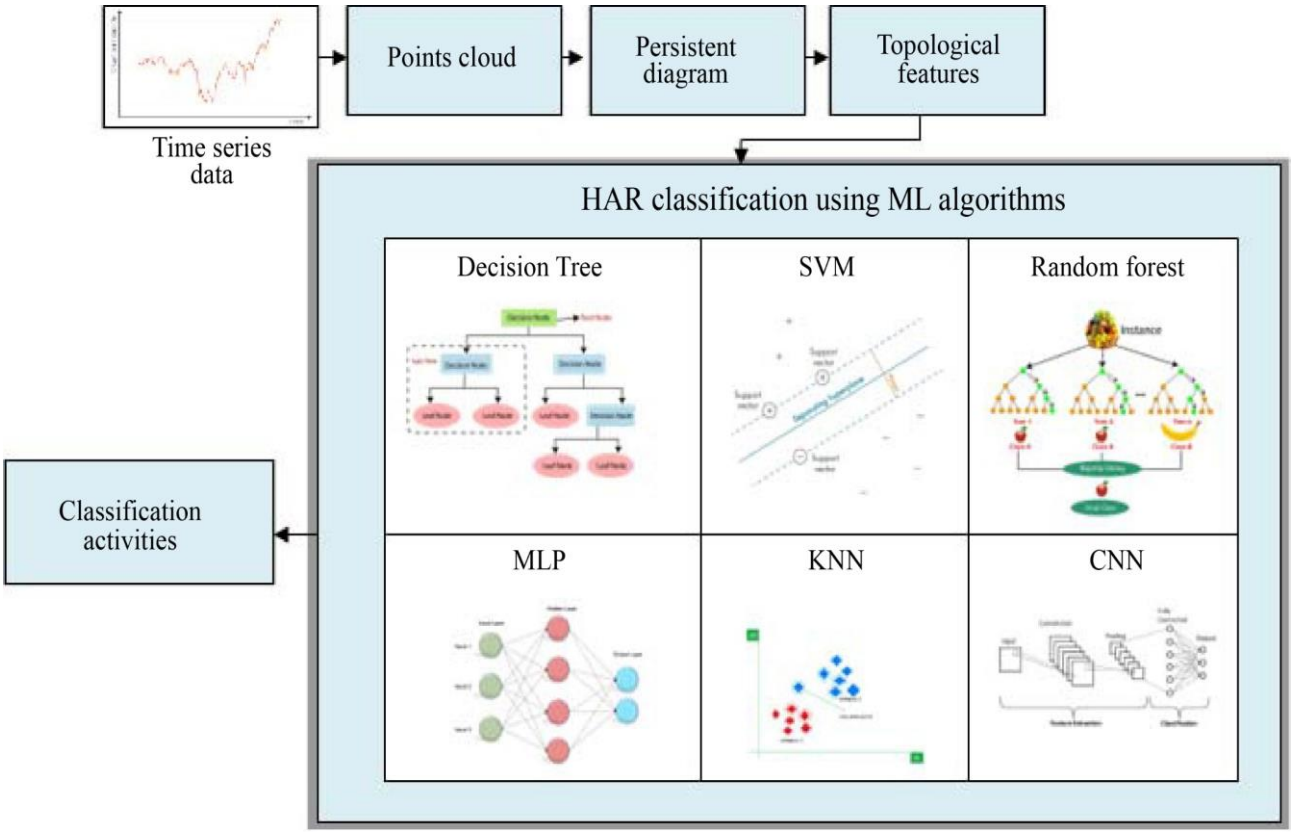

Fig. 1 Architectural model of the proposed HAR model

3.1. Topological Data

A set of points in, named a point cloud, can be transformed into a simplified complex, for instance, the Vietoris-Rips complex. A sequence of rising sub-complexes is formed, and several holes and their lifespan is computed and visualized as a so-called diagram or persistence in a filtration procedure. The barcode is a compilation of intervals, wherein interval lengths stand for the whole life span. The persistence illustration is a group of points, wherein the point's coordinates are the birth and death times of holes. Using cloud point, these 2-dimensional illustrations visualize global geometrical properties of the multidimensional shapes formed by the point cloud. The advantages of TDA rely on its capability for extracting global structure from local information and its consistency in perturbations. And in high-dimensional data analysis, the TDA is successful. During any physical activity (for instance, a martial arts approach), consider measurements coming from the position sensors [7]. The notations employed are represented as follows:S represents some measurements for each sensor, Qrepresents the number of sensors;$k_{cds}$is the c^{th} coordinate of the position of d^{th} the sensor in timet_s, wherein, $c = 0,\ldots,2, d = 1,\ldots,Q, and s = 1,\ldots,S$;

$$u_r = \{t_s, k_{01s}, k_{11s}, k_{21s}, k_{02s}, k_{12s}, k_{22s}, \ldots, k_{0Qs}, k_{1Qs}, k_{2Qs}\} \quad (1)$$

The point cloud that indicates the martial arts approach is stated as follows:

$$Z = \{u_r \in \Re^{3Q+1} : s = 1,\ldots,S\} \quad (2)$$

In the filtration procedure, a point cloud is transmitted into a nested family of simplified complexes in TDA. By persistence diagrams or barcodes, the persistent homology of the filtered, simplified complex (holes live span in the complex) is visualized. Using the point clouds $P_1$and $P_2$the Wasserstein distance or bottleneck can be computed between their barcodes to measure the similarity of martial arts approaches.

3.2. Topological Features

The utilization of a multi-scale approach reveals that persistence diagrams contain significant topological information about the input data [22]. To carry out the learning tasks, like regression, classification, or clustering, the

aforesaid descriptors can be utilized. Persistence diagrams are not appropriate for traditional ML approaches because of their representation as a multiset.

A distinctive approach is to reduce these descriptors into features in a Banach space, as performed with Betti curves, persistence images, and landscapes.

3.2.1. Betti Curve

The Betti curve$b_n: J \to B$ of a barcode $A = \{(a_m . b_m)\}_{m \in J}$represents a function that returns for every step $l \in J$, the count of bars (a_m, b_m)that comprise$l$ [8].

$$l \leftrightarrow \#\{(a_m, b_m), l \in (a_m, b_m)\} \quad (3)$$

3.2.2. Persistence Landscape

The r^{th} persistence landscape of a barcode represents the function $\alpha_r: B \to (0, \infty)$, wherein $\alpha_r(z)$represents the r^{th}highest value of $\{f_{(a_l,b_l)}(z)\}_{l=1}^{n}$.

$$f_{(a_l,b_l)}(z) = \begin{cases} 0 if z \notin (a,b) \\ z - a if z \in \left(a, \frac{a+b}{2}\right) \\ -z + b if z \in \left(\frac{a+b}{2}, b\right) \end{cases} \quad (4)$$

The parameter r is named layer. The curves achieved by setting $r = 1$and $r \in \{1,2\}$are considered [8].

3.2.3. Persistent Entropy

By taking Shannon entropy of the lifetime of persistence of all cycles, the persistent entropy of a barcode, which is a real number, is extracted:

$$P^E(A) = \sum_{l=1}^{n} \frac{i_l}{P(b)} log\left(\frac{i_l}{P(b)}\right) \quad (5)$$

Wherein $i_l := b_l - a_l \quad P(b) = i_1 +, \ldots, + i_n$exhibits summation of all persistence [8].

3.2.4. Wasserstein Amplitude

The Wasserstein amplitude of order $q$represents Pq the norm of a vector of point distances to the diagonal based on the Wasserstein distance [8]:

$$A^w = \frac{\sqrt{2}}{2} \left(\sum_l (b_l - a_l)^q\right)^{\frac{1}{q}} \quad (6)$$

where, $q = 1,2$

3.2.5. Bottleneck Distance

Considering$q$ the Wasserstein amplitude definition, the Bottleneck amplitude is obtained as follows:

$$B_l = \frac{\sqrt{2}}{2} sup(b_l - a_l) \quad (7)$$

4. HAR Classification using ML Approaches

This section presents a brief elucidation of all of the ML classification approaches presented in the proposed work.

4.1. KNN

To resolve both the regression techniques and classification, the KNN is mainly utilized, which is considered a supervised ML approach. Fresh data can be speedily organized into distinct groupings by means of the KNN approach. The KNN approach utilizes feature similarity to evaluate the values of any new data points.

In data, the distance between each example and a query is estimated, and K examples, which are nearer to the query, subsequently choose a label with the maximum frequency in the scenario of classification or the scenario of regression (average the labels). To utilize every training tuple, an n-dimensional pattern space is employed. The KNN classifier inspects the pattern space closest to the unrecognized tuple among the k-training tuples [9].

4.2. MLP

In several types of applications, the MLP model is extensively employed for ANN approaches. It has various levels of cover-up, as well as an input and output layer. This framework is frequently favoured for the MLP approach because of its efficiency and practicality in several applications. The function that ascertains the neuron activity must be differentiable as well as non-reducing to present a soft non-linearity. Moreover, two diverse transfer functions were used, such as hyperbolic tangent (tanh) [10]:

$$F(\lambda) = \frac{1}{1+e^{-\lambda}} \# \quad (8)$$

The log-sigmoid is given by:

$$F(\lambda) = \frac{2}{1+e^{-2\lambda}} - 1 \quad (9)$$

For mapping vectors, the neural network is mainly responsible. The most important aspiration is to regulate the parameters; thus, real output$x_p$intimately approximates the equivalent observed output $c_p \; p = 1, \ldots, P$. By reducing a few forms of error cost, the training process relies.

The fundamental BB is exploited during the course of analysis in conjunction with two individual training approaches (Levenberg-Marquardt BB and Bayesian regularization BB). Any transfer function is not posed by the primary layer; however, the hidden layer undergoes the application of sigmoid functions. Additionally, the output layer is constructed with the utilization of linear transfer functions, which enables it to generate precise predictions concerning the problems. Figure 2 represents the architectural model of MLP.

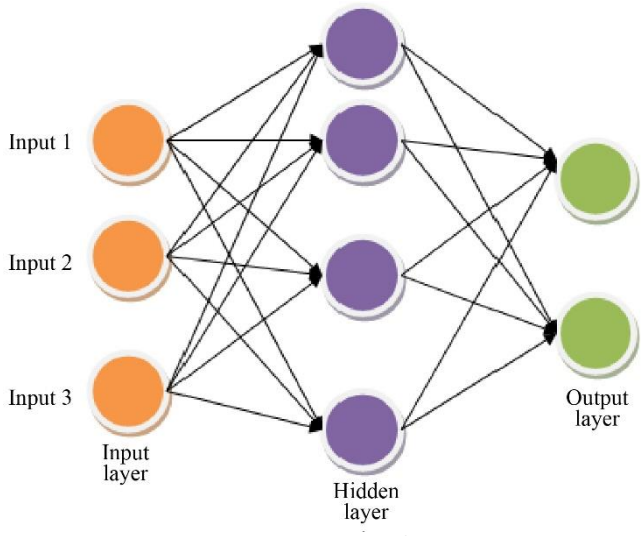

Fig. 2 Architecture diagram of MLP model

4.3. Decision Tree

To carry out the regression and classification tasks, a DT is used, which is a supervised learning strategy. It is generally utilized for classification. Moreover, a DT has branch nodes, roots, and leaf nodes, which are the same as the tree, with every node that indicates an attribute or characteristic, every branch indicates a rule or decision, and every leaf indicates an outcome. Moreover, the decision tree algorithm is utilized to divide the features. Also, the division is examined to observe if it is the most appropriate for the individual classes at each node. For a decision, a decision tree is a graphical design that permits the attainment of all the possible answers on the basis of present circumstances. Mainly, it concentrates on only one query, and a tree is divided into subtrees on the basis of the answer. The most important benefit of using the DT is that it is very effective for classification and regression issues, with the simplicity of interpretations, and the capability to fill in unfinished data in attributes with the maximum probable value. Also, it has the ability to handle quantitative and categorical values, and it has better effectiveness because of the effectiveness of the tree traversal model. The most important drawback faced by the DT is the overfitting issue, and the solution for it is the Random Forest, which is an ensemble modelling approach [9].

4.4. Random Forest

RF is an ensemble technique that creates numerous classifiers and groups their outcomes. Multiple CART trees are generated by the RF. Generally, CART is in with the nodes that comprise a complete learning sample. In RF, every tree will cast a binary decision tree, which is designed by dividing data in a node into child nodes frequently, voting for a few inputs, subsequently, the classifier output is ascertained by the maximum voting of the trees [11]. High-dimensional data is handled by the RF, and it employs a huge number of trees in the ensemble. A few significant principles of RF are a) RF is an effective model to estimate missing data, b) it has an approach, WRF, to balance error in imbalanced data, and finally, it calculates the significance of variables employed in classification.

4.5. Support Vector Machine

To deal with the regression and classification issues, the SVMs are extensively employed in supervised learning. The predominant intent of SVM is to determine an optimal decision or line to classify the n-dimensional space into parts; thus, the consecutive points might be categorized expediently. These boundaries are called hyperplanes. Moreover, the structured, semi-structured, and unstructured data are handled by the SVM. In data type, kernel functions solve the complexities. This technique is partitioned into two classifications: non-linear and linear data. The kernel functions and mathematical programming are the two most important executions of the SVM model. A hyperplane separates data points of diverse types within a higher-dimensional space [9].

4.6. CNN

From convolution operations, the word CNN was designed. In the CNN framework, the convolutional layer plays a significant role, as it is the module that performs feature extraction. Mainly, the layer comprises both non-linear and linear operations, which are an activation function and a convolution operation [12]. In addition, a filter is applied by convolution operations to secure spatial relationships among pixels by utilizing the learning features. During the convolution operation, the convolved feature, activation map, and feature map are employed to explain the data generated.

The kernel values are automatically enhanced as a CNN is trained to efficiently detect features of new inputs. The number of filters used (such as the depth dimension value), the border padding with zeros (zero padding), and the count of pixels by which the filter slides (such as the stride) determine the feature map size [12]. This setup is to be identified and recognized where they are positioned in the input data. The main aim of utilizing a convolution layer to train a CNN approach is to set up the most effective and appropriate kernels for a given task to be ascertained on the basis of the training dataset presented. During training, kernels are functions that are only learned automatically in the convolution layer.

5. Result and Analysis

The developed approach was executed by using the Python programming language, and analysis was performed on the "HAR [13]" dataset by considering the metrics, such as accuracy, precision, recall, and F1-score.

5.1. Dataset Description

HAR [13]: The dataset encompasses GPS, acceleration, gyroscope, magnetic field, light, and sound level information associated with various activities, including climbing stairs up and down, sitting, running/jogging, lying, standing, jumping,

and walking. These activities were carried out by fifteen subjects, and for each activity, data were recorded concurrently from on-body positions, such as the upper arm, chest, head, forearm, shin, thigh, and waist. Figure 3 demonstrates the confusion matrix and it is a table depicting the performance of the classifier, where classes are denoted from A to S. Each classes corresponds to specific activities, like "A" represents walking, "B" represents Jogging, "C represents stairs, "D" represents Sitting, "E" represents Standing, "F" represents Typing, "G represents Brushing Teeth, "H" represents Eating Soup, "I" represents Eating Chips, "J" represents Eating Pasta, "K" represents Drinking from Cup, "L" represents Eating Sandwich, "M" represents Kicking Soccer Ball", "O" represents Playing Catch w/Tennis Ball", "P" represents Dribblinlg (Basketball)", "Q" represents Writing", "R" represents Clapping", "S" represents Folding Clothes". Figure 3 (a) demonstrates the phone accel score that yields an accuracy of 78%. Figure 3 (b) exhibits the phone gyro score personal that yields an accuracy of 85%. Figure 3 c) illustrates the watch accel score that yields an accuracy of 98%. Figure 3(d) exhibits the watch gyro score personal that yields an accuracy of 97%. Figure 3 (e) shows the phone accelerometer score impersonal. Figure 3 (f) displays the phone gyro score impersonal, Figure 3 (g) demonstrates the watch accel score impersonal, and Figure 3 (h) exhibits the watch gyro score impersonal.

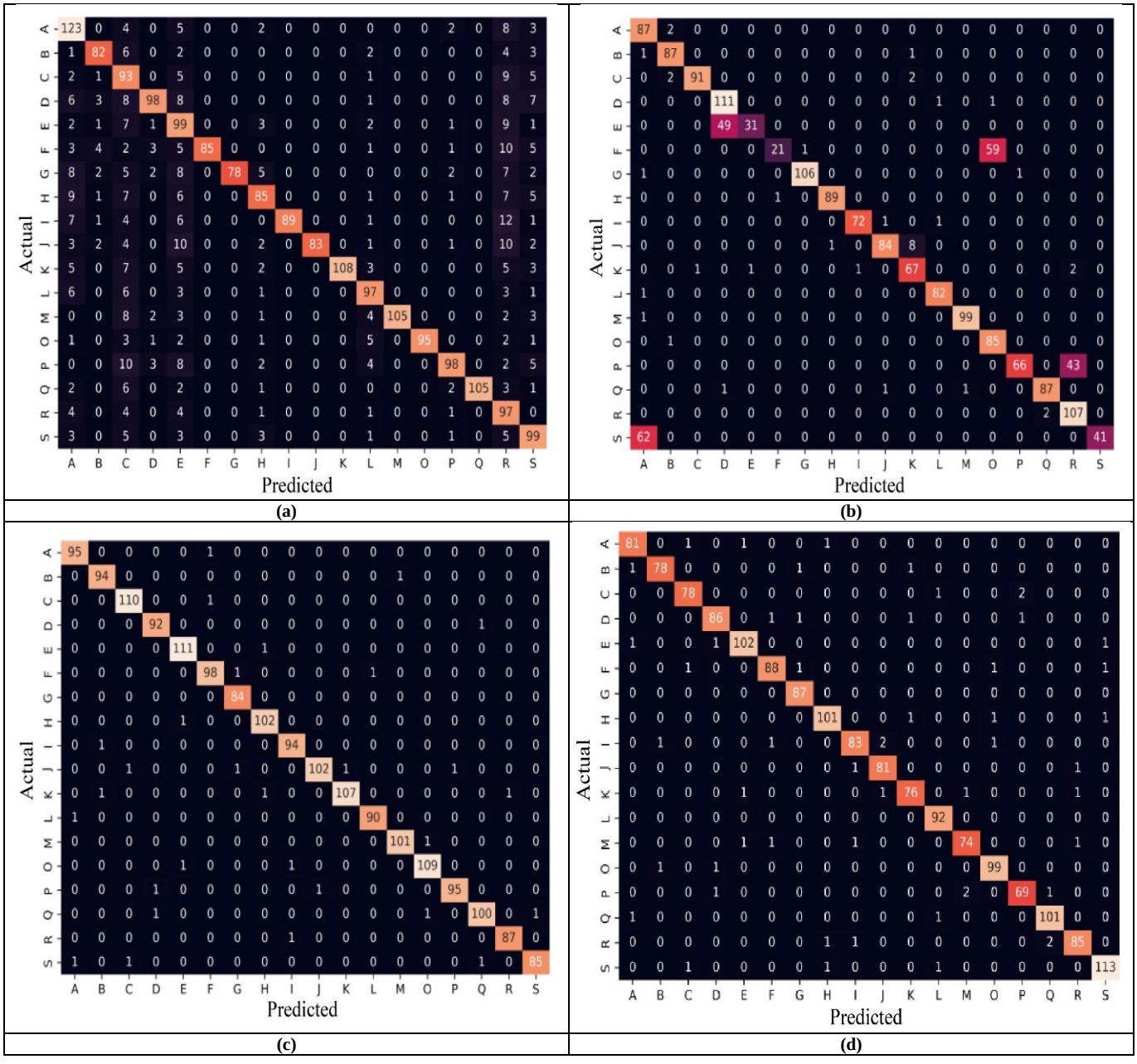

(a) **(b)**

(c) **(d)**

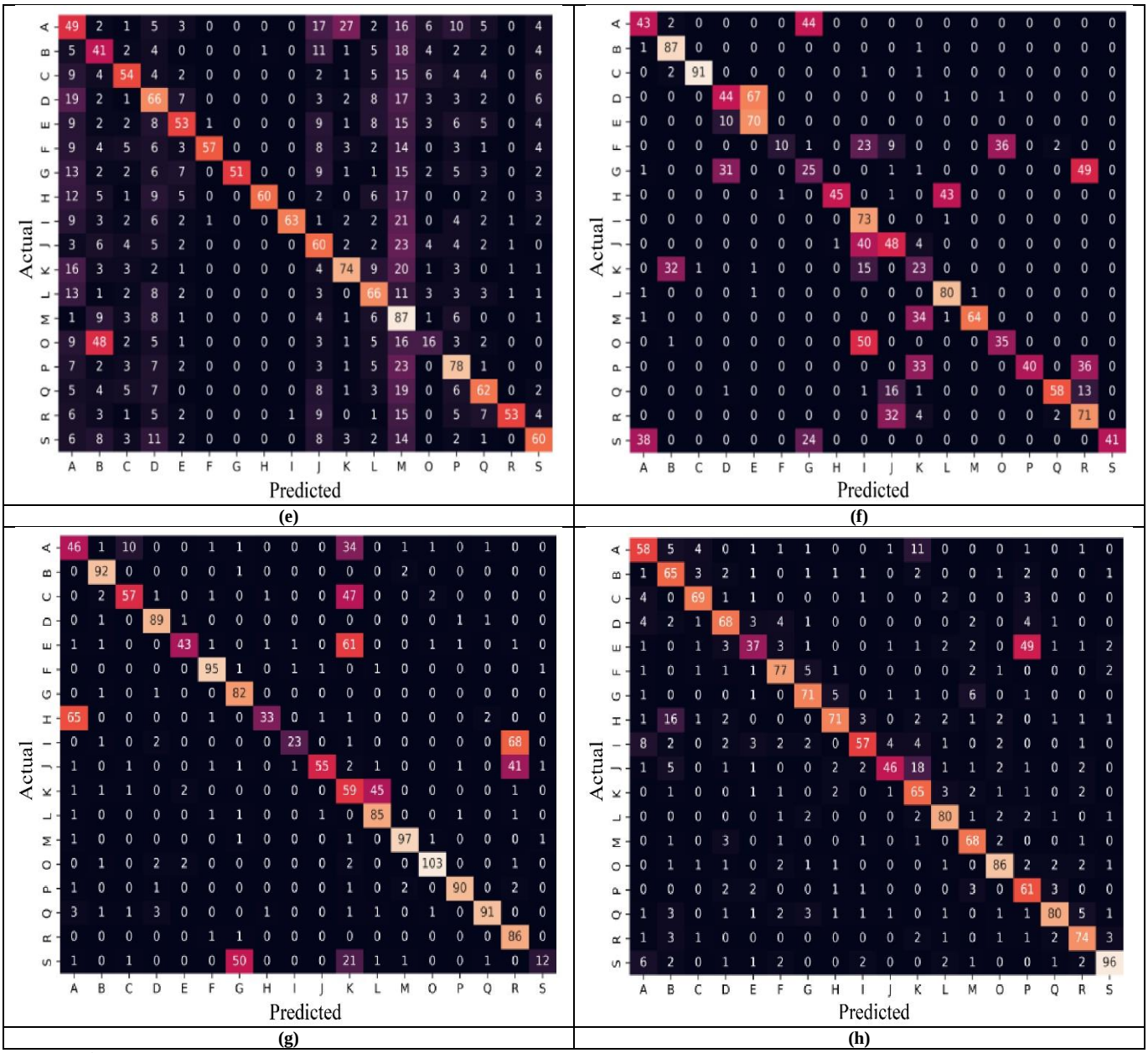

Fig. 3 Confusion matrix (a) Phone accel score personal, (b) Phone gyro score personal, (c) watch accel score personal, (d) Watch gyro score personal, (e) Phone accel score impersonal, (f) Phone gyro score impersonal, (g) Watch accel score impersonal, and (h) Watch gyro score impersonal.

5.2. Comparative Analysis

Figure 4 specifies the analysis of phone accel score personnel regarding accuracy, recall, precision, and F1-score. Figure 4 (a) specifies analysis for accuracy, CNN attained a maximal accuracy of 77.8%, whereas other methods, such as Decision tree attained 73.6% accuracy, MLP attained 74% accuracy, SVM attained 74.9% accuracy, KNN attained 73.4% accuracy, and RF attained 75.6% accuracy, for k-fold=14. Figure 4 (b) states evaluation for recall, the CNN attained the maximal value of 77.6%, whereas other approaches, such as Decision tree, MLP, SVM, KNN, and RF attained minimal recall values of 62, 65.7, 71.3, 61.3, and 75.7 for k-fold=5. Figure 4 (c) expresses evaluation for precision, the CNN attained the maximal precision value of 95.1, whereas other methods, like Decision tree, MLP, SVM, KNN, and RF attained a minimal precision value of 74.8, 63.5, 73.4, 68.3, and 88.7 for k-fold=15. Figure 4 (d) signifies analysis for F1 score, CNN attained a maximal F1-score of 74.49, whereas Decision tree, MLP, SVM, KNN, and RF attained a minimum F1-score of 52.46, 58.88, 19.61, 52.14, and 64.58, for k-fold=10.The analysis of phone gyro score personnel regarding accuracy, recall, precision, and F1-score was illustrated in Figure 5. Figure 5 (a) signifies accuracy. When k-fold was 6, the accuracy of the CNN model was 72.6%, whereas the accuracy of the CNN was raised to 85.2% when k-fold was 15.

Figure 5 (b) signifies recall; the CNN attained the maximal recall value of 96.5, whereas other approaches, such as Decision tree, MLP, SVM, KNN, and RF, attained a minimal recall value of 58.8, 59.7, 60.4, 61.1, and 78.8, for k-fold=15. Figure 5 (c) expresses precision; the CNN attained the maximal precision value of 85.3, whereas the Decision Tree, MLP, SVM, KNN, and RF attained a minimal precision value of 62.9, 67.3, 57.8, 66.3, and 75.8 for k-fold=14. Figure 5 (c) expresses F1-score, Decision tree, MLP, SVM, KNN, RF attained minimal F1-score value of 41.94, 42.09, 32.44, 33.81, 48.87, 63.67 for k-fold=10. Meanwhile, CNN attained the maximal F1-score value of 63.67.

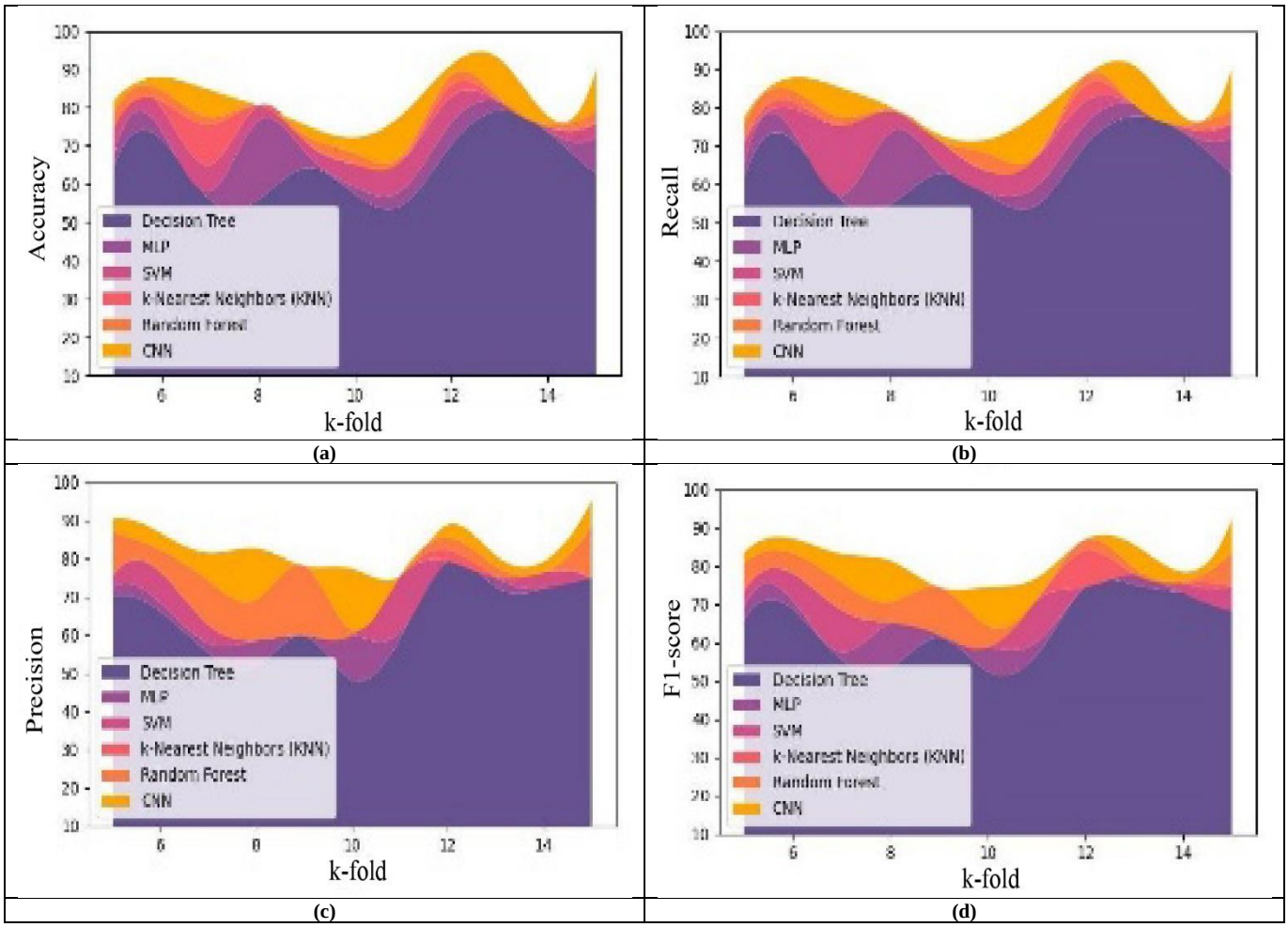

Fig. 4 Analysis of phone accel score, personal (a) Accuracy, (b) Recall, (c) Precision, and (d) F1-score.

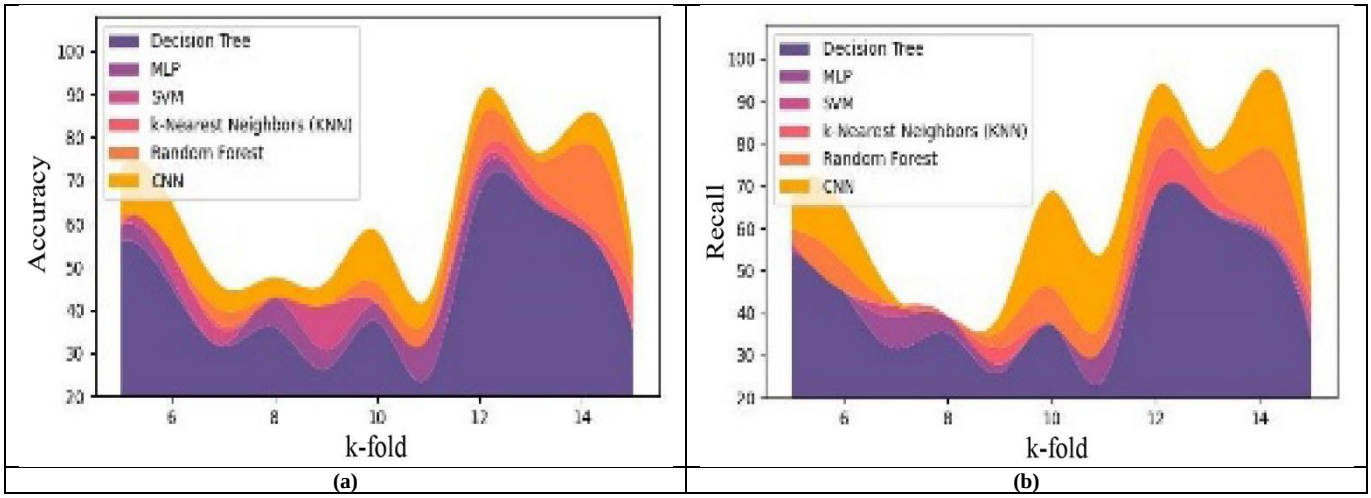

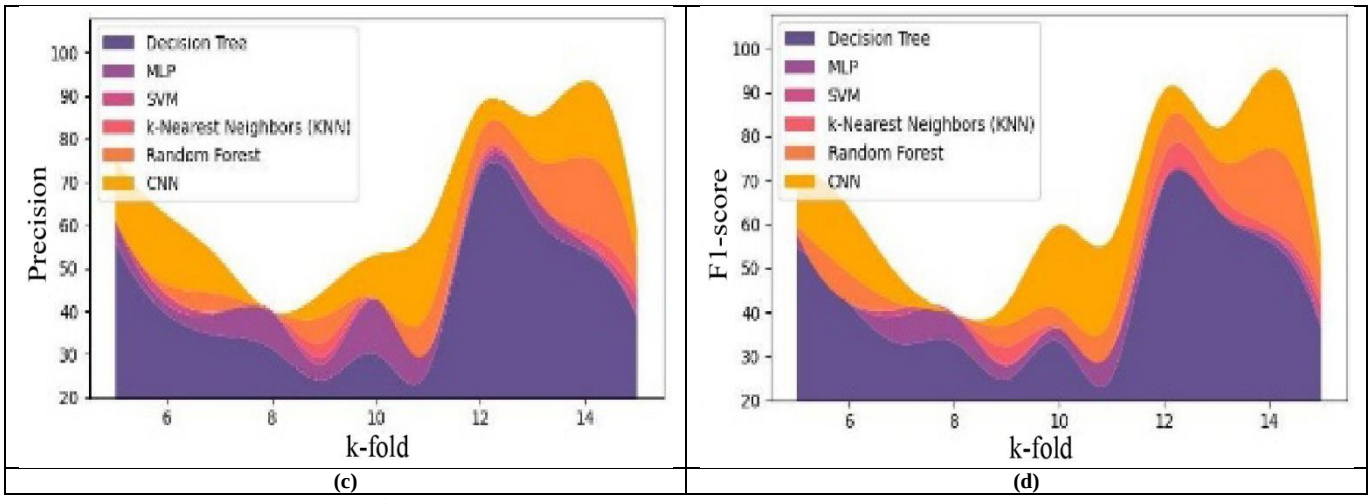

(c) (d)

Fig. 5 Analysis of phone gyro score personal (a) Accuracy, (b) Recall, (c) Precision, and (d) F1-score.

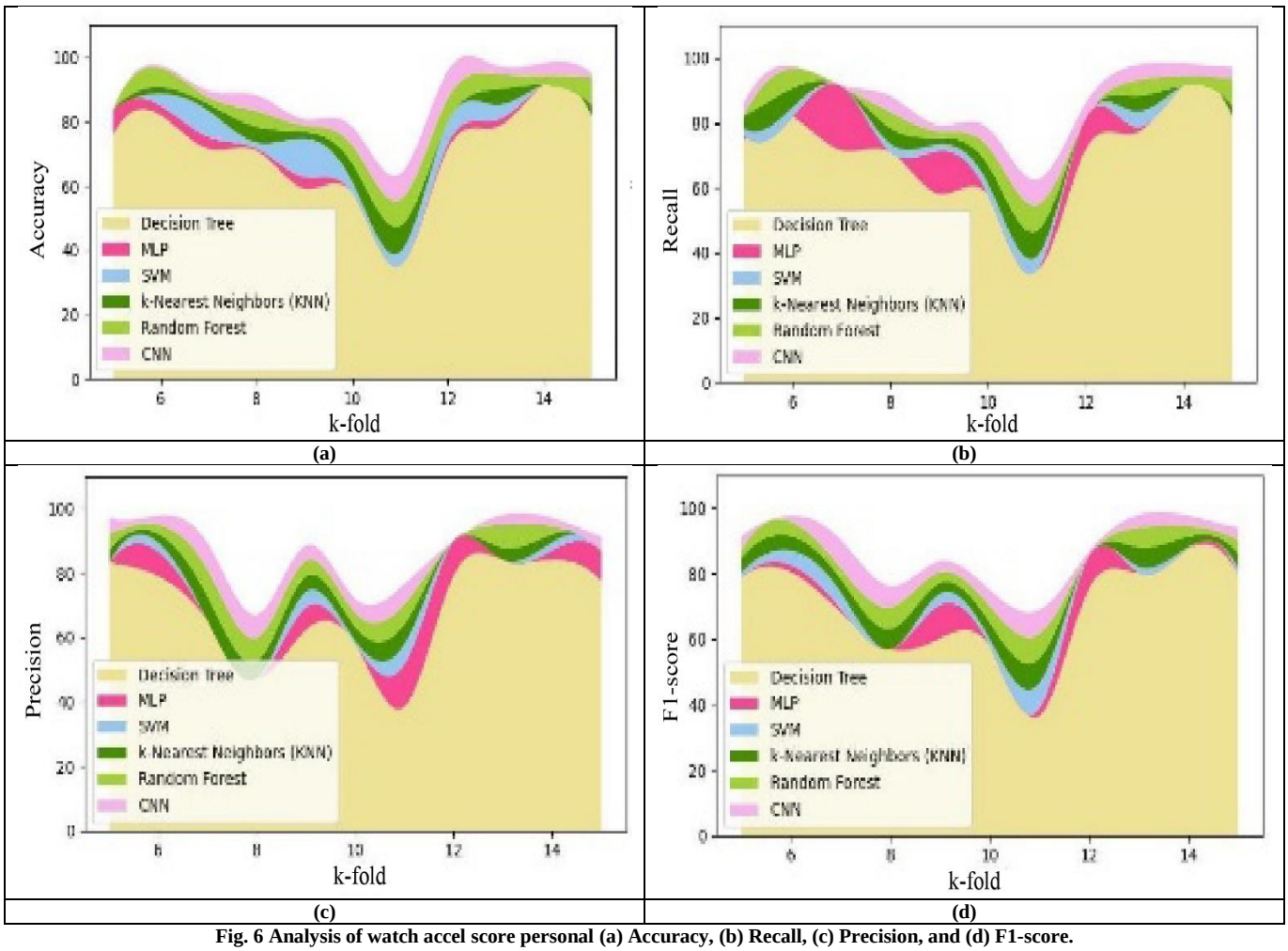

(a) (b)

(c) (d)

Fig. 6 Analysis of watch accel score personal (a) Accuracy, (b) Recall, (c) Precision, and (d) F1-score.

The analysis of watch accel score personnel regarding accuracy, recall, precision, and F1-score was exhibited in Figure 6. Figure 6 (a) states evaluation based on accuracy, the CNN attained the maximal accuracy value of 98.3%, whereas other methods, namely Decision tree, MLP, SVM, KNN, and RF attained a minimal accuracy value of 91.5%, 82.7%, 86.6%, 90.5%, and 94.4%, for k-fold=15. Figure 6 (b) states the analysis for recall. The CNN attained a maximal recall value of 86.2, whereas the Decision Tree, MLP, SVM, KNN, and RF attained a minimal recall value of 74.3, 76.2, 78.2,

82.2, and 82.2 for k-fold=6. Figure 6 (c) specifies the analysis for precision. When CNN attained the maximal precision value of 87.1, Decision tree, MLP, SVM, KNN, and RF attained the minimal precision value of 79.1, 89.9, 88.7, 87.5, and 86.3 for k-fold=13. Figure 6 (d) states the analysis for the F1-score. For k-fold=6, CNN attained the maximal F1-score value of 97.55, whereas Decision tree, MLP, SVM, KNN, and RF attained the minimal F1-score value of 80.32, 82.48, 86.94, 91.35, and 95.69, respectively. The analysis of watch gyro score personnel regarding accuracy, recall, precision, and F1-score is exhibited in Figure 7.

As interpreted in Figure 7 (a), the CNN attained an accuracy value of 97.2, whereas the MLP attained only 76.4 for k-fold=15. Moreover, the CNN attained a recall value of 87.9, while the Decision tree and MLP attained only 64.1 and 48.3 for k-fold=10, as stated in Figure 7(b). Moreover, the CNN attained a precision value of 90.9, but the precision value of the Decision tree was 83.5, and the precision of SVM was 85.8 for k-fold=15, which is specified in Figure 7 (c). The CNN attained an F1-score value of 85.7, whereas the F1-score of the Decision tree was 65.71, and RF was 77.96 for k-fold=5, which is expressed in Figure 7 (d).

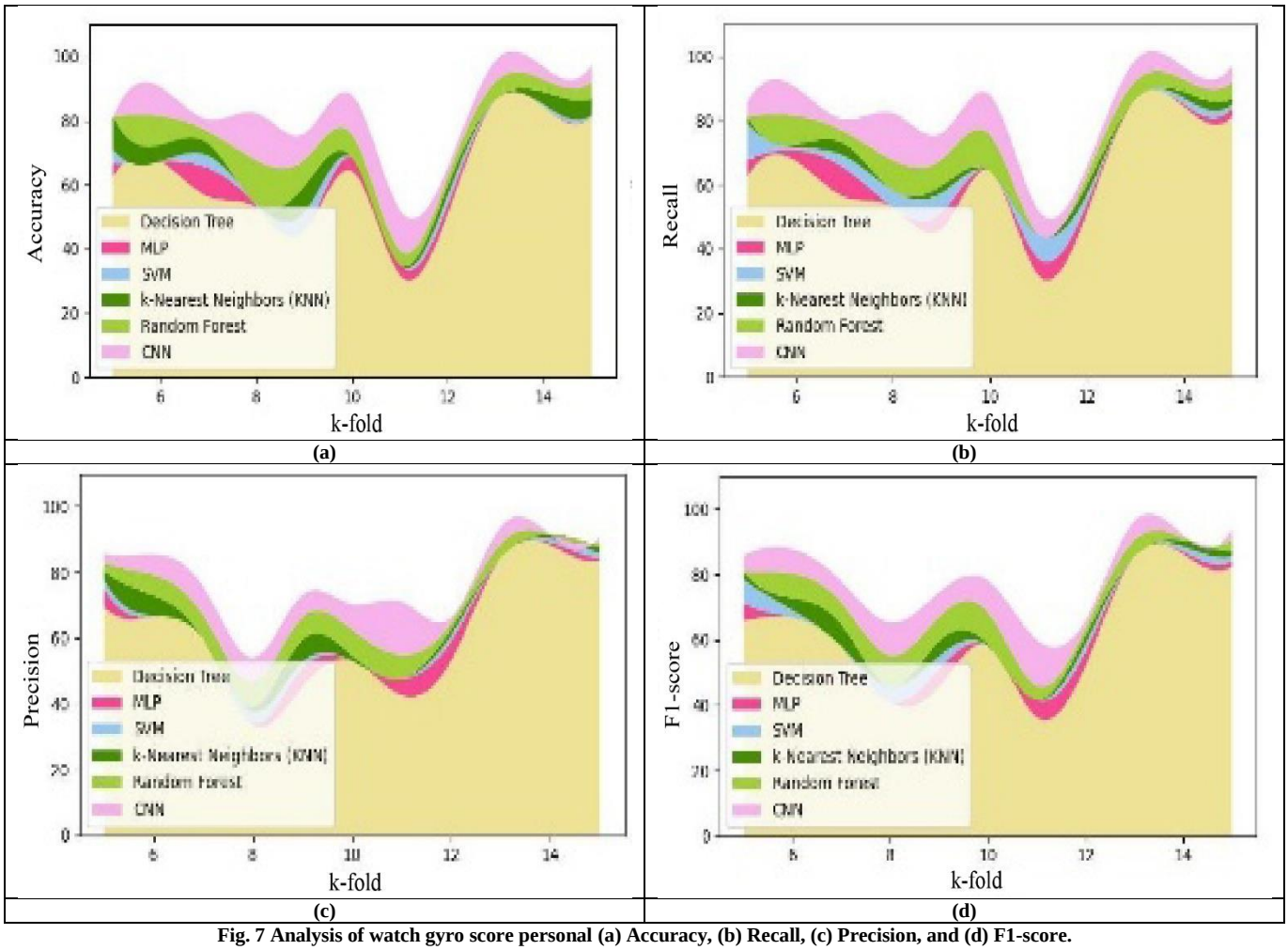

Fig. 7 Analysis of watch gyro score personal (a) Accuracy, (b) Recall, (c) Precision, and (d) F1-score.

Analysis of phone accelerometer score in terms of accuracy, recall, precision, and F1-score was illustrated in Figure 8. Figure 8 (a) states the analysis for accuracy. For k-fold=15, when CNN attained a maximal accuracy value of 12.5, Decision tree, MLP, SVM, KNN, and RF attained a minimal accuracy value of 7, 6.1, 8.7, 9.3, and 5.9. Figure 8(b) expresses the evaluation for recall. The CNN attained the maximal recall value of 11.2, while Decision tree, MLP, SVM, KNN, and RF attained a minimal recall value of 12.1, 9.4, 9.6, 9.8, and 10, for k-fold=10. Figure 8 (c) expresses evaluation for precision; the precision value of the Decision tree was 7.9, and the precision value of CNN was 14.3 for k-fold=15. Figure 8 (d) expresses the evaluation for the F1-score. The F1-score of the KNN was 13.37, the F1-score of RF was 10.49, but CNN attained a maximal F1-score of 15.84 for k-fold=5.

Analysis of phone gyro scores in terms of accuracy, recall, precision, and F1-score was exhibited in Figure 9. Figure 9 (a) expresses the assessment for accuracy. CNN attained a maximal accuracy of 30.2, whereas the accuracy of the Decision tree was 12.4, MLP was 19.4, SVM was 10.5, KNN was 10.4, RF was 20.3, for k-fold=15. Figure 9 (b)

states the evaluation for recall. The CNN attained a maximal recall of 10.1, while the recall of the Decision tree was only 7.6, and that of MLP was only 5.9 for k-fold=10. Additionally, the precision value of CNN was 40.5, but the precision of RF was only 33.3 for k-fold=14, as stated in Figure 9 (c).

The CNN attained a maximal F1-score value of 32.45, whereas other strategies, like Decision tree, MLP, SVM, KNN, RF, attained a minimal F1-score value of 16.35, 16.97, 18, 18.34, 22.98, for k-fold=15, which is specified in Figure 9 (d).

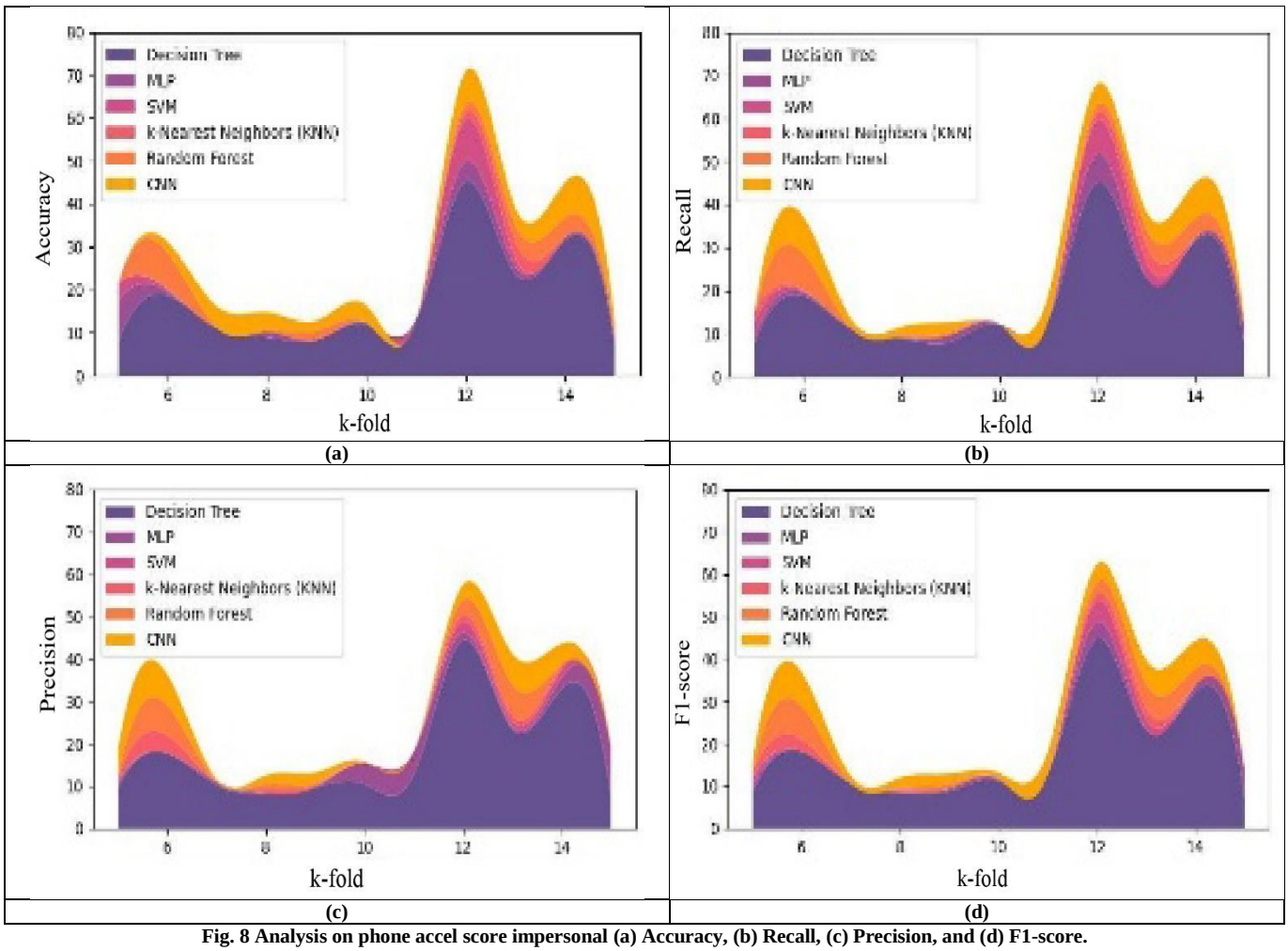

Fig. 8 Analysis on phone accel score impersonal (a) Accuracy, (b) Recall, (c) Precision, and (d) F1-score.

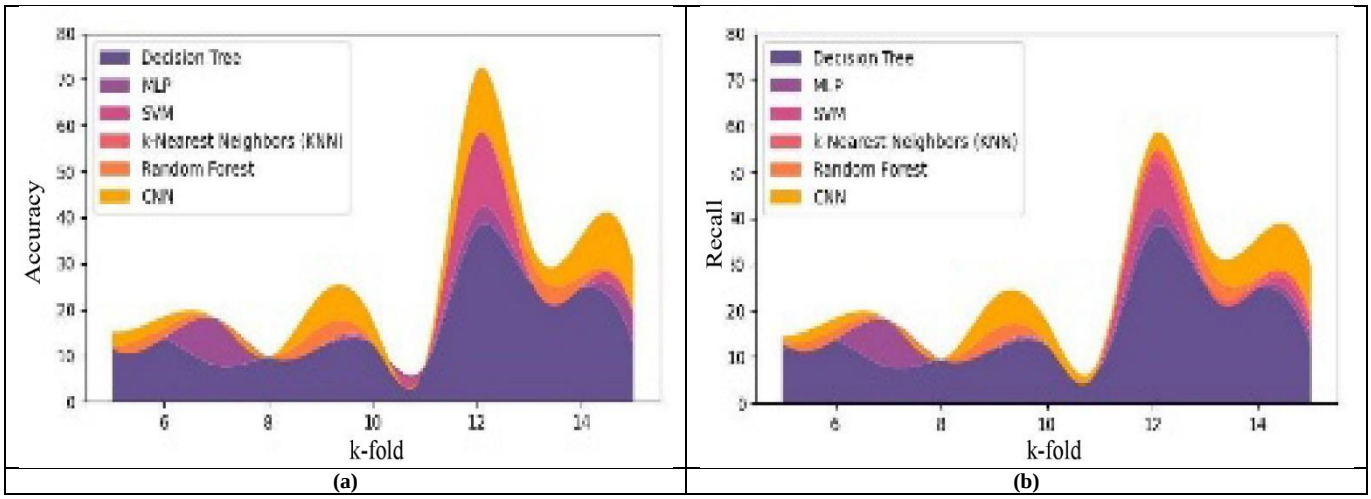

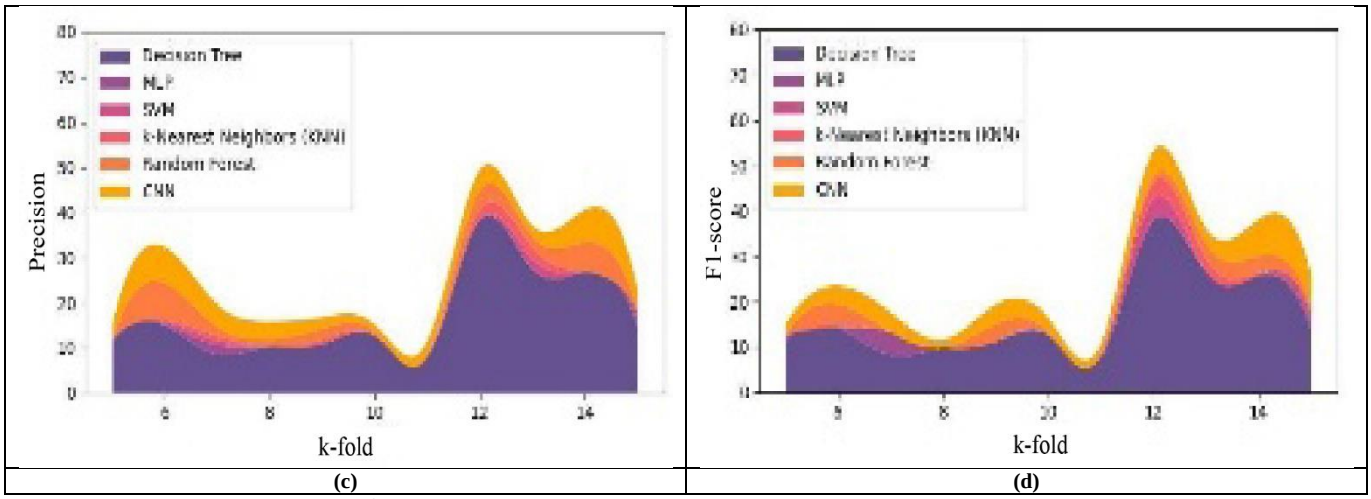

(c) **(d)**

Fig. 9 Analysis of phone gyro score impersonal (a) Accuracy, (b) Recall, (c) Precision, and (d) F1-score.

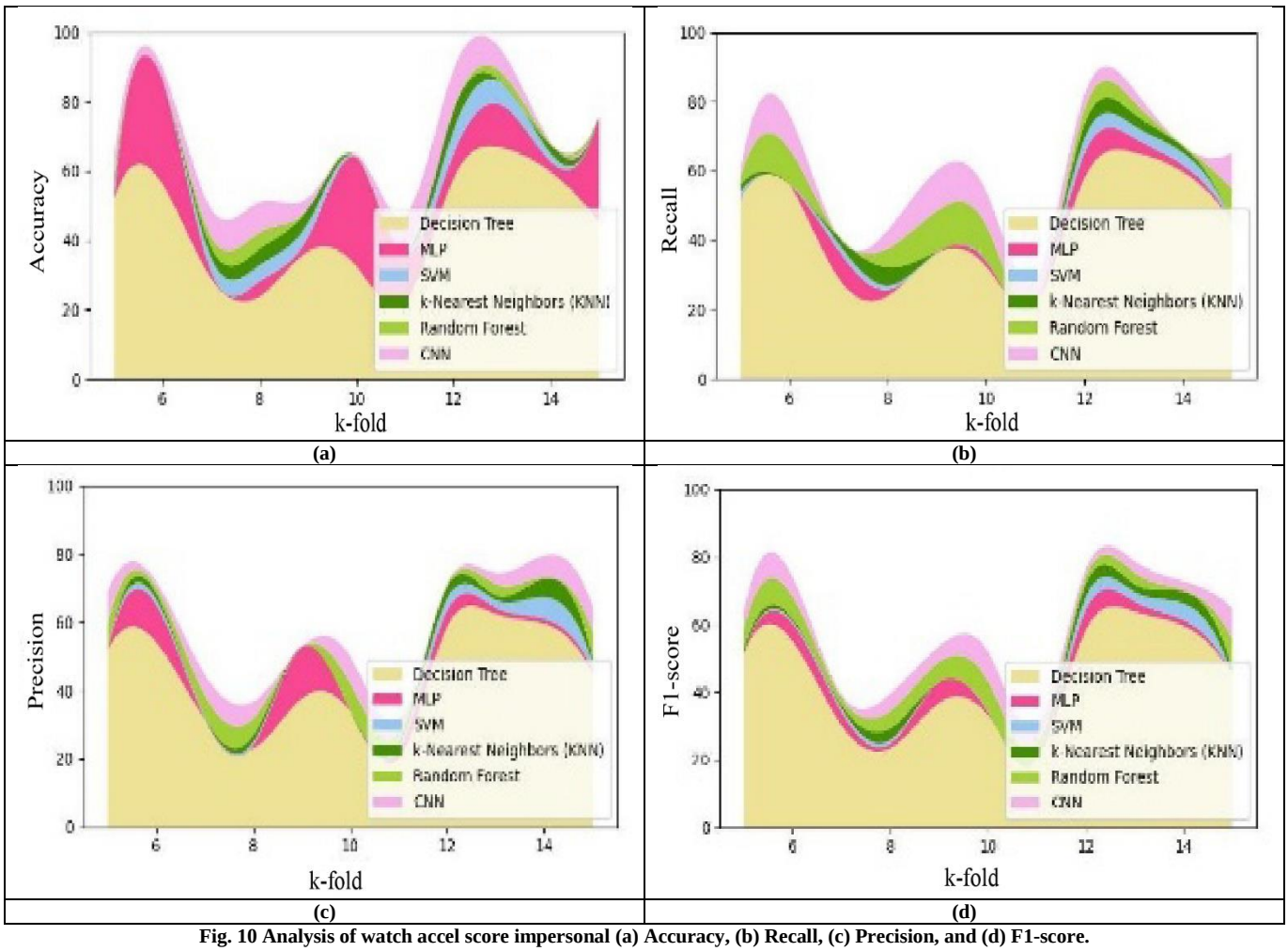

(a) **(b)**

(c) **(d)**

Fig. 10 Analysis of watch accel score impersonal (a) Accuracy, (b) Recall, (c) Precision, and (d) F1-score.

Analysis of the watch accel score in terms of accuracy, recall, precision, and F1-score was illustrated in Figure 10. Figure 10 (a) expresses the evaluation for accuracy. CNN reached a maximal accuracy value of 65, whereas other approaches, like Decision tree, MLP, SVM, KNN, and RF, attained a minimal accuracy value of 52.1, 53.4, 55.3, 57.1, and 59.2, for k-fold=5. Moreover, the CNN attained a maximal recall of 54.1, whereas the Decision tree attained the minimal recall of 32.4 for k-fold=10, which is stated in Figure 10 (b).

Additionally, the precision of CNN was 64.4, while the precision of the decision tree was 44.8, and that of MLP was 46, and SVM was 47.8 for k-fold=15, which is specified in Figure 10 (c). Figure 10 (d) states the analysis based on the F1-score. The F1-score of the Decision tree was a minimal value of 51.59, and the F1-score of CNN was a maximum of 62.4 for k-fold=5.Analysis of watch gyro scores, impersonal for accuracy, recall, precision, and F1-score, was shown in Figure 11. Compared to Decision tree, MLP, SVM, KNN, and RF, CNN reached a maximal accuracy of 56.6%, for k-fold=10. Meanwhile, Decision tree, MLP, SVM, KNN, and RF attained minimum accuracy of 28, 29.7, 30.4, 31.8, and 59.2, which is portrayed in Figure 11 (a). Figure 11 (b) portrays the analysis for recall. The CNN achieved a maximum recall of 67.7, whereas Decision Tree, MLP, SVM, KNN, and RF achieved a minimum recall of 46.9, 54.9, 45.6, 46.3, and 57, respectively, for k-fold = 15. Moreover, the precision of the Decision tree was only 48, while that of CNN was 66.2 for k-fold=15, which is stated in Figure 11 (c). Figure 11 (d) specifies the analysis for the F1-score. The F1-score of the Decision tree was only 46.05, but the F1-score of CNN was maximal with a range of 61 for k-fold=5.

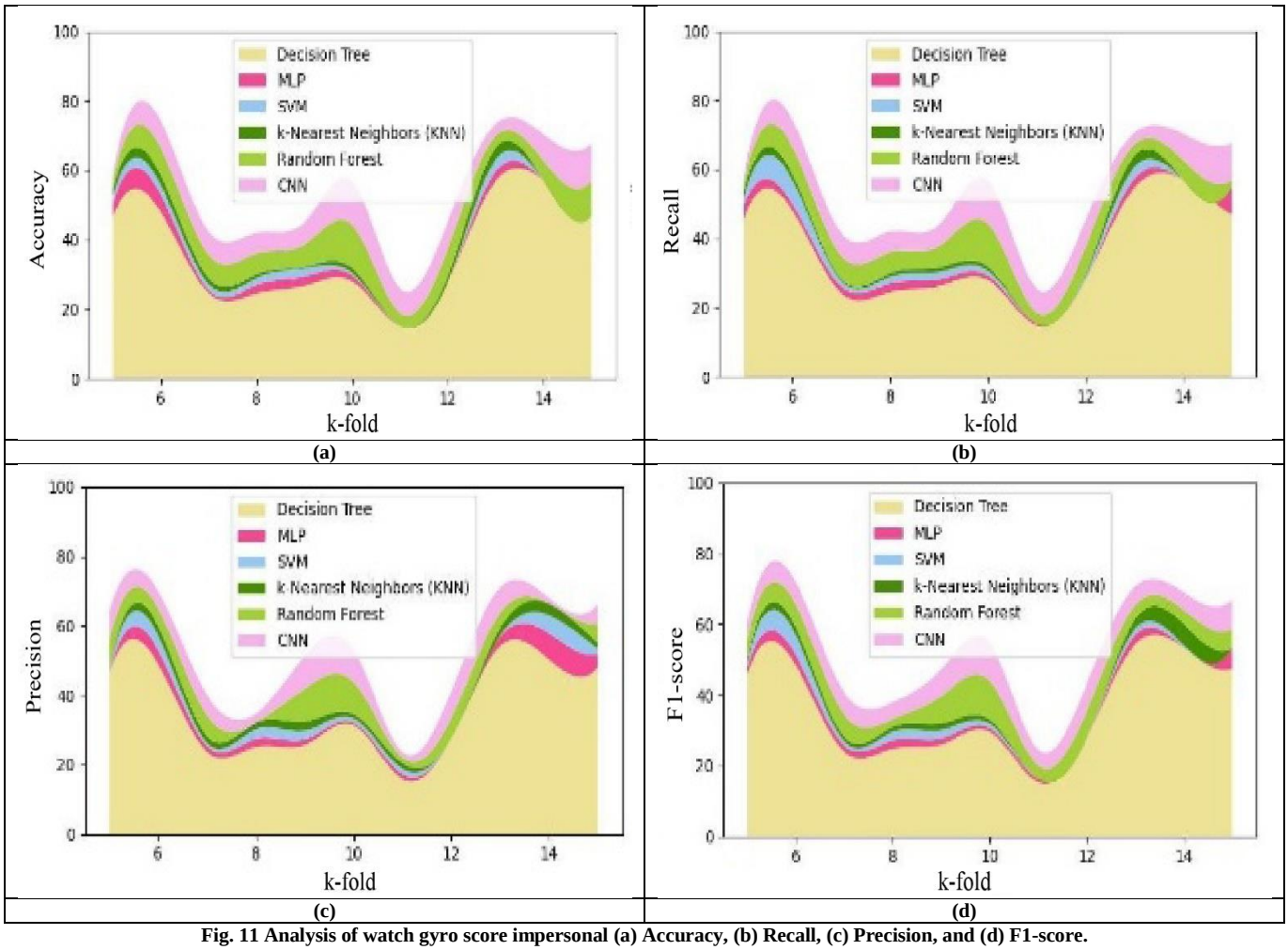

Fig. 11 Analysis of watch gyro score impersonal (a) Accuracy, (b) Recall, (c) Precision, and (d) F1-score.

Table 1 illustrates the comparative analysis regarding accuracy, recall, precision, and F1-score. Here, phone accel score_personal,phone_gyro_score_personal, watch_accel_score_personal,watch_gyro_score_personal,phone_accel_score_impersonal,phone_gyro_score_impersona, watch_accel_score_impersonal,and watch_gyro_score_impersonal.

Table 1. Comparative analysis

phone_accel_score_personal						
	Decision Tree	MLP	SVM	KNN	RF	CNN
Accuracy	62.7	72.3	75.95	58.5	79.3	90.1
Recall	62.7	72.3	75.95	58.5	79.3	90.1
Precision	74.8	63.5	73.4	68.3	88.7	95.1

F1-score	68.22	67.61	74.65	63.02	83.74	92.53
phone_gyro_score_personal						
	Decision Tree	MLP	SVM	KNN	RF	CNN
Accuracy	58.8	50.3	51.4	61.1	78.8	85.2
Recall	58.8	59.7	60.4	61.1	78.8	96.5
Precision	53.8	55.9	44.1	58.3	75.9	93.5
F1-score	56.19	57.74	50.98	59.67	77.32	94.98
watch_accel_score_personal						
	Decision Tree	MLP	SVM	KNN	RF	CNN
Accuracy	91.5	82.7	86.6	90.5	94.4	98.3
Recall	91.5	82.7	86.6	90.5	94.4	98.3
Precision	83.9	86.9	89.4	91.9	94.4	96.9
F1-score	87.54	84.75	87.98	91.19	94.4	97.59
watch_gyro_score_personal						
	Decision Tree	MLP	SVM	KNN	RF	CNN
Accuracy	81.2	76.4	81.6	86.8	92	97.2
Recall	81.2	83.9	85.1	86.8	92	97.2
Precision	83.5	84.1	85.8	87.5	89.2	90.9
F1-score	82.33	84	85.45	87.15	90.58	93.94
phone_accel_score_impersonal						
	Decision Tree	MLP	SVM	KNN	RF	CNN
Accuracy	7	6.1	8.7	9.3	5.9	12.5
Recall	7	11.1	10.7	9.3	5.9	12.5
Precision	7.9	19.5	15.7	11.9	8.1	14.3
F1-score	7.42	14.15	12.73	10.44	6.83	13.34
phone_gyro_score_impersonal						
	Decision Tree	MLP	SVM	KNN	RF	CNN
Accuracy	12.4	19.4	10.5	10.4	20.3	30.2
Recall	12.2	14.2	16.5	18.2	19.9	29.6
Precision	14.7	16.4	18.3	13.1	18.1	23.1
F1-score	16.35	16.97	18	18.35	22.98	32.45
watch_accel_score_impersonal						
	Decision Tree	MLP	SVM	KNN	RF	CNN
Accuracy	45.3	75.8	65.3	54.8	44.3	53.8
Recall	45.3	23.3	33.8	45.3	54.8	65.3
Precision	44.8	46	47.8	49.2	56.8	64.4
F1-score	45.3	35.64	44.54	49.60	48.99	58.99
watch_gyro_score_impersonal						
	Decision Tree	MLP	SVM	KNN	RF	CNN
Accuracy	46.9	24.9	35.6	46.3	57	67.7
Recall	46.9	54.9	45.6	46.3	57	67.7
Precision	48	51.8	53.4	55	60.6	66.2
F1-score	47.44	53.3	49.19	50.28	58.74	66.94

Table 2 presents the analysis for 12 classes, including phone acceleration score personal, phone gyroscope scores personal, watch acceleration score personal, watch gyroscope score personal, phone acceleration score impersonal, phone gyroscope scores impersonal, watch acceleration score impersonal, and watch gyroscope score impersonal. For label A, phone_accel_score_personal attained an accuracy of 0.836, whereas watch_gyro_score_impersonal attained an accuracy of 0.68. For the S class, phone_accel_score_personal achieved an accuracy of 0.825, while phone_gyro_score_personal achieved 0.398, watch_accel_score_personal achieved 0.966, and watch_gyro_score_personal achieved 0.958. Meanwhile, for the same class, phone_accel_score_impersonal achieved an accuracy of 0.5, phone_gyro_score_impersonal achieved an accuracy of 0.398, watch_accel_score_impersonal achieved an accuracy of 0.136, and watch_gyro_score_impersonal achieved an accuracy of 0.813. Here, the overall analysis states that the accuracy of watch_gyro_score_personal attained better accuracy than the other classes.

Table 2. Accuracy of the labels

Lables	phone_accel_score_personal	phone_gyro_score_personal	watch_accel_score_personal	watch_gyro_score_personal	phone_accel_score_impersonal	phone_gyro_score_impersonal	watch_accel_score_impersonal	watch_gyro_score_impersonal
A	0.836	0.978	0.990	0.964	0.34	0.483	0.479	0.68
B	0.82	0.978	0.990	0.963	0.41	0.978	0.968	0.802
C	0.8017	0.853	0.991	0.963	0.465	0.958	0.514	0.852
D	0.705	0.982	0.989	0.956	0.475	0.389	0.957	0.756
E	0.785	0.388	0.991	0.971	0.421	0.875	0.384	0.352
F	0.714	0.259	0.98	0.956	0.479	0.123	0.95	0.837
G	0.655	0.981	1	1	0.428	0.231	0.976	0.816
H	0.697	0.99	0.99	0.971	0.492	0.5	0.320	0.683
I	0.735	0.971	0.989	0.943	0.521	0.986	0.242	0.648
J	0.703	0.903	0.962	0.9759	0.508	0.516	0.519	0.554
K	0.7831	0.931	0.972	0.95	0.536	0.319	0.536	0.813
L	0.829	0.988	0.989	1	0.564	0.964	0.934	0.870
M	0.820	0.99	0.99	0.949	0.680	0.64	0.951	0.872
O	0.856	0.988	0.982	0.98	0.144	0.407	0.928	0.852
P	0.742	0.606	0.979	0.742	0.591	0.367	0.928	0.656
Q	0.861	0.967	0.971	0.981	0.508	0.645	0.882	0.777
R	0.866	0.982	0.988	0.955	0.473	0.651	0.977	0.83
S	0.825	0.398	0.966	0.958	0.5	0.398	0.136	0.813

5.3. Discussion

The improved outcomes are mainly attributed to combining topology-based data analysis with varied ML algorithms, facilitating efficient capture of spatial and temporal structures. Persistent diagrams offered resilient features lost by conventional methods. Moreover, classifying classical and ML classifiers helped pick optimal models for the dataset. Feature selection also simplified the model without affecting accuracy, making the method feasible for resource-limited devices. These elements collectively added to the enhanced performance relative to current practice.

6. Conclusion and Future Work

In this work, a topology-based HAR method was designed by utilizing several machine learning (ML) techniques, namely Random Forest, KNN, SVM, CNN, Decision Tree, and MLP. From the time series data, topological features, like persistent landscape, Betti curve, Persistent Entropy, Persistent images, and Wasserstein amplitude were extracted. By employing the extracted features, various ML methods, Random Forest, SVM, CNN, Decision Tree, KNN, and MLP were used to recognize the human activities. Finally, the experimentation was performed using the accuracy, loss, precision, recall, and F-measure. Moreover, overall analysis indicates that the CNN model achieved superior accuracy, recall, precision, and F1-score than other models, with the values of 98.3, 98.3, 96.9, and 98. Moreover, for the watch_accel_score_personal label, the method achieved the maximum accuracy of about 99%. DL techniques may be investigated in the future to augment the performance of HAR systems. Such sophisticated models are proficient in learning intricate patterns in activity data more efficiently compared to conventional approaches. Another possibility is including a wider selection of evaluation metrics, e.g., specificity, false positive rate, and false negative rate, so that there is a more complete determination of model performance and both accurate and inaccurate classifications are better analyzed and corrected.

Nomenclature

MoCap	Motion capture
RNN	Recurrent Neural Network
IMU	Internal Measurement Units
AI	Artificial intelligence
TDA	Topological data analysis
ML	Machine Learning
HMM	Hidden Markov Model
SVMs	Support Vector Machines
E2E	end-to-end
DL	Deep Learning
INN	Inception Neural Network
TCA-GCN	Temporal-Channel Aggregation Graph Convolutional Network
LSTM	Long Short-Term Memory
GAP	Global Average Pooling layer
HAR	Human Activity Recognition
DNN	Deep Neural Network
WRF	Weighted Random Forest
CART	Classifications and Regression
MLP	Multilayer Perceptron
RF	Random forest
TDA	Topological Data Analysis

DT	Decision Tree	EE	Extreme Edge
SOM	Self-Organizing Maps	IFTT	Football Team Training Algorithm
FL	Federated Learning	MST	Minimum Spanning Trees
IoT	Internet-of-Things	BB	Backpropagation

References

[1] Cheng Xu et al., "Innohar: A Deep Neural Network for Complex Human Activity Recognition," *IEEE Access*, vol. 7, pp. 9893-9902, 2019. [CrossRef] [Google Scholar] [Publisher Link]

[2] Kun Xia, Jianguang Huang, and Hanyu Wang, "LSTM-CNN Architecture for Human Activity Recognition," *IEEE Access*, vol. 8, pp. 56855-56866, 2020. [CrossRef] [Google Scholar] [Publisher Link]

[3] Shengqin Wang et al., "Skeleton-based Action Recognition via Temporal-Channel Aggregation," *arXiv Preprint*, pp. 1-13, 2022. [CrossRef] [Google Scholar] [Publisher Link]

[4] Javier Lamar Leon et al., "Topological Features for Monitoring Human Activities at Distance," *International Workshop on Activity Monitoring by Multiple Distributed Sensing*, Stockholm, Sweden, pp. 40-51, 2014. [CrossRef] [Google Scholar] [Publisher Link]

[5] I-Cheng Chang, and Chung-Lin Huang, "The Model-based Human Body Motion Analysis System," *Image and Vision Computing*, vol. 18, no. 14, pp. 1067-1083, 2000. [CrossRef] [Google Scholar] [Publisher Link]

[6] Umar Islambekov, Monisha Yuvaraj, and Yulia R. Gel, "Harnessing the Power of Topological Data Analysis to Detect Change Points," *Environmetrics*, vol. 31, no. 1, pp. 1-26, 2020. [CrossRef] [Google Scholar] [Publisher Link]

[7] Marcin Żelawski, and Tomasz Hachaj, "The Application of Topological Data Analysis to Human Motion Recognition," *Technical Transactions*, vol. 118, no. 1, pp. 1-10, 2021. [CrossRef] [Google Scholar] [Publisher Link]

[8] Adélie Garin, and Guillaume Tauzin, "A Topological "Reading" Lesson: Classification of MNIST using TDA," *2019 18th IEEE International Conference on Machine Learning and Applications (ICMLA)*, Boca Raton, FL, USA, pp. 1551-1556, 2019. [CrossRef] [Google Scholar] [Publisher Link]

[9] Vraj Sheth, Urvashi Tripathi, and Ankit Sharma, "A Comparative Analysis of Machine Learning Algorithms for Classification Purpose," *Procedia Computer Science*, vol. 215, pp. 422-431, 2022. [CrossRef] [Google Scholar] [Publisher Link]

[10] Abdulrahman Sumayli, and Saad M. Alshahrani, "Modeling and Prediction of Biodiesel Production by Using Different Artificial Intelligence Methods: Multi-Layer Perceptron (MLP), Gradient Boosting (GB), and Gaussian Process Regression (GPR)," *Arabian Journal of Chemistry*, vol. 16, no. 7, pp. 1-14, 2023. [CrossRef] [Google Scholar] [Publisher Link]

[11] Mohammed Khalilia, Sounak Chakraborty, and Mihail Popescu, "Predicting Disease Risks from Highly Imbalanced Data Using Random Forest," *BMC Medical Informatics and Decision Making*, vol. 11, no. 1, pp. 1-13, 2011. [CrossRef] [Google Scholar] [Publisher Link]

[12] Leila Mohammadpour et al., "A Survey of CNN-based Network Intrusion Detection," *Applied Sciences*, vol. 12, no. 16, pp. 1-34, 2022. [CrossRef] [Google Scholar] [Publisher Link]

[13] *Human Activity Recognition*, Data and Web Science Group, 2025. [Publisher Link]

[14] Frédéric Chazal, and Bertrand Michel, "An Introduction to Topological Data Analysis: Fundamental and Practical Aspects for Data Scientists," Frontiers in Artificial Intelligence, vol. 4, pp. 1-28, 2017. [CrossRef] [Google Scholar] [Publisher Link]

[15] Milan Joshi, and Dhananjay Josh, "A survey of Topological Data Analysis Methods for Big Data in Healthcare Intelligence," *International Journal of Applied Engineering Research*, vol. 14, no. 2, pp. 584-588, 2019. [Google Scholar] [Publisher Link]

[16] Gregory D. Abowd et al., "Towards A Better Understanding of Context and Context-Awareness," *International Symposium on Handheld and Ubiquitous Computing*, Karlsruhe, Germany, pp. 304-307, 1999. [CrossRef] [Google Scholar] [Publisher Link]

[17] Ling Bao, and Stephen S. Intille, "Activity Recognition from User-Annotated Acceleration Data," *International Conference on Pervasive Computing*, Linz, and Vienna, Austria, pp. 1-17, 2004. [CrossRef] [Google Scholar] [Publisher Link]

[18] Diane Cook, Kyle D. Feuz, and Narayanan C. Krishnan, "Transfer Learning for Activity Recognition: A Survey," *Knowledge and Information Systems*, vol. 36, no. 3, pp. 537-556, 2013. [CrossRef] [Google Scholar] [Publisher Link]

[19] Charissa Ann Ronao, and Sung-Bae Cho, "Human Activity Recognition with Smartphone Sensors Using Deep Learning Neural Networks," *Expert Systems with Applications*, vol. 59, pp. 235-244, 2016. [CrossRef] [Google Scholar] [Publisher Link]

[20] Daniele Ravì et al., "A Deep Learning Approach to On-Node Sensor Data Analytics for Mobile or Wearable Devices," *IEEE Journal of Biomedical and Health Informatics*, vol. 21, no. 1, pp. 56-64, 2017. [CrossRef] [Google Scholar] [Publisher Link]

[21] Charissa Ann Ronao, and Sung-Bae Cho, "Deep Convolutional Neural Networks for Human Activity Recognition with Smartphone Sensors," *International Conference on Neural Information Processing*, Istanbul, Turkey, pp. 46-53, 2015. [CrossRef] [Google Scholar] [Publisher Link]

[22] Olympio Hacquard, "*From Topological Features to Machine Learning Models: A Journey through Persistence Diagrams*," Doctoral Dissertation, Paris-Saclay University, 2023. [Google Scholar] [Publisher Link]

[23] Sungjoon Park, Yoonseok Hwang, and Bohm-Jung Yang, "Unsupervised Learning of Topological Phase Diagram Using Topological Data Analysis," Physical Review B, vol. 105, no. 19, pp. 1-12, 2022. [CrossRef] [Google Scholar] [Publisher Link]

[24] Gunnar Carlsson et al., "Topological Data Analysis and Machine Learning Theory," *Proceeding Banff International Research Station Workshop*, pp. 1-11, 2012. [Google Scholar] [Publisher Link]

[25] Eric Cawi, Patricio S. La Rosa, and Arye Nehorai, "Designing Machine Learning Workflows with an Application to Topological Data Analysis," *PloS one*, vol. 14, no. 12, pp. 1-26, 2019. [CrossRef] [Google Scholar] [Publisher Link]

[26] Angelo Trotta et al., "Edge Human Activity Recognition Using Federated Learning on Constrained Devices," *Pervasive and Mobile Computing*, vol. 104, pp. 1-15, 2024. [CrossRef] [Google Scholar] [Publisher Link]

[27] Shiwen Lan et al., "Human Action Recognition based on MnasNet Optimized by Improved Version of Football Team Training Algorithm," *Biomedical Signal Processing and Control*, vol. 110, 2025. [CrossRef] [Google Scholar] [Publisher Link]

[28] Lingyue Hu et al., "Improving Human Activity Recognition via Graph Attention Network with Linear Discriminant Analysis and Residual Learning," *Biomedical Signal Processing and Control*, vol. 100, 2025. [CrossRef] [Google Scholar] [Publisher Link]

[29] Yan Yan et al., "Topological Nonlinear Analysis of Dynamical Systems in Wearable Sensor-Based Human Physical Activity Inference," *IEEE Transactions on Human-Machine Systems*, vol. 53, no. 4, pp. 792-801, 2023. [CrossRef] [Google Scholar] [Publisher Link]

[30] Yuxuan Zhou et al., "BlockGCN: Redefine Topology Awareness for Skeleton-Based Action Recognition," *2024 IEEE/CVF Conference on Computer Vision and Pattern Recognition (CVPR)*, Seattle, WA, USA, pp. 2049-2058, 2024. [CrossRef] [Google Scholar] [Publisher Link]

[31] Walaa N. Ismail et al., "AUTO-HAR: An Adaptive Human Activity Recognition Framework Using an Automated CNN Architecture Design," *Heliyon*, vol. 9, no. 2, pp. 1-20, 2023. [CrossRef] [Google Scholar] [Publisher Link]

[32] Hung-Cuong Nguyen et al., "Deep Learning for Human Activity Recognition on 3D Human Skeleton: Survey and Comparative Study," *Sensors*, vol. 23, no. 11, pp. 1-33, 2023. [CrossRef] [Google Scholar] [Publisher Link]